奨励金No.1496

高速視線焦点制御と高速画像処理に基づく広域高精細車載ビジョンシステム

平野　正浩
東京大学　助教

Onboard High-speed Vision System for Broad and High-definition Observation

Masahiro Hirano,
The University of Tokyo, Assistant Professor

本研究では、高速カメラに取り付けた電動ズームレンズと 2 軸ガルバノミラーを用いた新しいアクティブビジョンシステムである Falcon を提案する。このシステムは、近くから遠くまで広域かつ高精細なイメージングを可能とする。Falcon を駆動するために、マッピングベースの高精度キャリブレーション手法と効率的なビジュアルフィードバック手法を提案し、カーブミラーのトラッキングを実現することで提案システムの有効性を示した。

We propose a novel active vision system, called Falcon, that includes an electric zoom lens attached to a high-speed camera with a pair of galvanometer mirrors. This system enables high-resolution imagery of an object moving over a wide range, from near to far.

We also propose a new mapping-based calibration method and present a robust and lightweight visual feedback method for object tracking. We constructed a prototype and conducted tracking experiments in an indoor environment, which showed the superiority of our method. Additionally, we successfully demonstrated continuous and high-resolution imaging of a curved mirror on public roads while the vehicle was in motion.

1. 研究内容

1. Introduction

Sensing the surrounding environment is a fundamental function of robots, including autonomous vehicles. While recent advances in electronics have enabled the development of various sensors such as LiDAR and millimeter radar, vision sensors play an irreplaceable role due to their high capability in environmental recognition, which is widely appreciated in many vehicle applications.

Conventional onboard vision sensors observe the surrounding scene homogeneously with a fixed optical system, which inherently has a tradeoff between the measurement area and resolution. However, there is a contrast in importance in different parts of the surrounding environment. This suggests that by optically adjusting the measurement area according to the context of the surrounding environment, areas important for driving can be observed with high resolution, contributing to safer and more efficient automatic driving. For example, by focusing on a curved mirror, the system can observe a blind area around the corner in detail.

In this study, we introduce a novel active onboard vision system called *Falcon*, which overcomes the limitations of conventional systems by using a 2-axis galvano-mirror and variable optics with adjustable zoom and focal position (Fig. 1). This enables the continuous observation of a wide and distant area at high resolution, enabling safer and more efficient automatic driving. To ensure accurate and reliable performance, we developed a tracking mechanism that let Falcon to keep the object at the center of the field of view, even when the object's relative position changes rapidly owing to vehicle movement or the vibration. We also propose a novel mapping-based calibration method that ensures the accuracy and precision of the Falcon's performance, as well as a visual feedback method that utilizes the calibration data to optimize object tracking. We developed a prototype and successfully demonstrated the continuous tracking of a curved mirror as an example of an area in the surrounding environment while the ego vehicle was in motion.

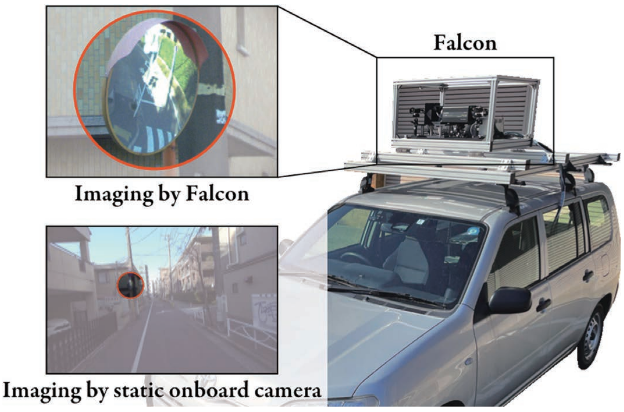

Fig. 1 Falcon enables high-resolution imagery of a moving object in a wide range from near to far.

2. Falcon: A Wide-and-deep Onboard Active Vision System

2.1. Components

The Falcon system comprises a dual-axis galvanometer mirror and an electrically controllable zoom lens equipped with a high-speed camera (internal camera), as shown in Fig. 2. The optical axis of the internal camera was carefully aligned to hit the center of the first mirror and is parallel to the axis of the second mirror. The internal camera observes the foreground scene by changing its gaze direction through a pair of reflections from the fast-tilting mirrors. In addition to the internal camera, two wide-angle video rate cameras (external cameras) were mounted on the Falcon system. These cameras observe the foreground scene to locate areas in environments where close observations are required.

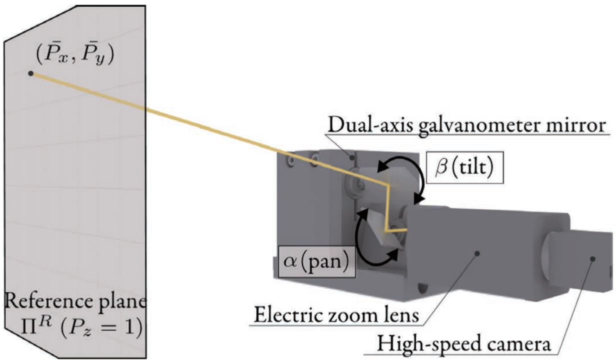

Fig. 2 Schematic drawing of Falcon.

2.2. Calibration

2.2.1. Model-based calibration

We calibrated the Falcon system using an optical model originally developed for a Saccade Mirror, which also comprises a pair of galvanometer mirrors. During the model-based calibration process, the zoom ratio (R_Z) was set to be constant. Prior to calibrating the Falcon, we first performed stereo calibration of the two wide-angle cameras. To achieve this, we placed a large calibration board in front of the system and made the Falcon scan the board to record the mirror angles, along with the recognized corner point's 3D position (determined through triangulation) and its projected point onto the internal camera. We then calculated the calibration parameters through optimization using the model and measurements. Using these parameters, we obtain a model-based projection

$$\pi\left(\mathrm{P};\mathrm{R}_\mathrm{Z}\right)$$

which maps a point P on a reference plane Π_R to a point p on an image plane Π_I, where Π_R is a plane parallel to $P_x - P_y$ plane, that is, $P_z = 1$. However, the accuracy of the model-based calibration was insufficient chiefly because of modeling errors.

2.2.2. Mapping-based calibration

To further improve calibration accuracy, we propose a method to refine the projection through an additional calibration process. First, we captured a pair of images of the calibration board using wide-angle cameras to obtain the 3D positions $\left(P_x, P_y, P_z\right)$ of the corner points of the board, which were placed in front of the system.

For each corner point, we set the mirror angles α (pan) and β (tilt) to observe the corner point at the center using parameters from the model-based calibration and we adjusted the angles delicately so that the center of the image coincided with the corner point. We then obtained a refined mapping $M:\left(\overline{\mathrm{P}_\mathrm{x}},\overline{\mathrm{P}_\mathrm{y}}\right)\rightarrow\left(\alpha,\beta\right)$, where $\left(\overline{\mathrm{P}_\mathrm{x}},\overline{\mathrm{P}_\mathrm{y}}\right)=\left(\mathrm{P}_\mathrm{x}/\mathrm{P}_\mathrm{z},\mathrm{P}_\mathrm{y}/\mathrm{P}_\mathrm{z}\right)$ is the projected corner point on the reference plane Π_R. This mapping accurately corresponded to the gaze direction relative to the angles of the mirror. After repeating this process several times to obtain a collection of mappings M_i, we approximated the mappings M_i by a pair of continuous functions μ_α and μ_β using cubic polynomial surfaces with bisquare robust estimators.

$$\left(\alpha,\beta\right)=\mu\left(\overline{\mathrm{P}_\mathrm{x}},\overline{\mathrm{P}_\mathrm{y}}\right)=\left(\mu_\alpha\left(\overline{P_x},\overline{P_y}\right),\mu_\beta\left(\overline{P_x},\overline{P_y}\right)\right)$$

2.3. Control

An active vision system commonly employs a PID controller to adjust the mirror's angle to minimize the distance to the center. However, adjusting the control parameters can lead to instability. In this work, we propose a novel mapping-based visual feedback method for active vision systems that maximize the use of accurate calibration. Let $\mathrm{p}^\mathrm{t}\in\Pi_\mathrm{I}$ be the location of the target at time T where the mirror angles are α, β, and let $\mathrm{p}^\mathrm{c}\in\Pi_\mathrm{I}$ be the center of the image.

New mirror angles α', β' are required to drive the mirrors to capture the object at the center, which is equivalent to deriving the location of the object on the reference plane $\mathrm{P}^\mathrm{t}=\mu^{-1}\left(\alpha',\beta'\right)$. However, we cannot directly obtain P^t from p^t with μ^{-1} because μ describes the relationship between the mirror angles and a point on the reference plane, which is always mapped to the center of the image.

To address this issue, we assumed the accuracy of the model-based calibration. It is assumed that the distances between points $\mu^{-1}\left(\alpha',\beta'\right)$, $\mu^{-1}\left(\alpha,\beta\right)$ are approximately equal to the distances between points $\pi^{-1}\left(\mathrm{p}^\mathrm{t};\mathrm{R}_\mathrm{Z}\right),\pi^{-1}\left(\mathrm{p}^\mathrm{c};\mathrm{R}_\mathrm{Z}\right)$.

$$\mu^{-1}\left(\alpha',\beta'\right)-\mu^{-1}\left(\alpha,\beta\right)\simeq\pi^{-1}\left(\mathrm{p}^\mathrm{t};\mathrm{R}_\mathrm{Z}\right)-\pi^{-1}\left(\mathrm{p}^\mathrm{c};\mathrm{R}_\mathrm{Z}\right)$$

where R^Z is the zoom ratio at time T, which is updated in real time. The approximate mirror angles are obtained as follows:

$$\begin{aligned}\left(\alpha',\beta'\right)&=\mu\left(\mathrm{P}^\mathrm{t}\right)\\&=\mu\left(\mathrm{P}^\mathrm{c}+\left(\mathrm{P}^\mathrm{t}-\mathrm{P}^\mathrm{c}\right)\right)\\&=\mu\left(\mu^{-1}\left(\alpha,\beta\right)+\mu^{-1}\left(\alpha',\beta'\right)-\mu^{-1}\left(\alpha,\beta\right)\right)\\&\simeq\mu\left(\mu^{-1}\left(\alpha,\beta\right)+\pi^{-1}\left(\mathrm{p}^\mathrm{t};\mathrm{R}_\mathrm{Z}\right)-\pi^{-1}\left(\mathrm{p}^\mathrm{c};\mathrm{R}_\mathrm{Z}\right)\right)\end{aligned}$$

We refer to this as mapping-based feedback control. Note that we approximate the inverse of μ

in the same manner as μ because μ is injective. Because all the functions are algebraic and precomputable, the computational cost is low. In addition, unlike PID control, no parameters need to be tuned by the users, which is advantageous for practical use.

3. Curved mirror tracking

3.1. Scenario

We demonstrated the use of Falcon for curved mirror tracking on public roads as an application of intelligent vehicles. Curved mirrors are commonly used in Japan to help drivers observe blind spots in their vehicles. To conduct tests, we firmly mounted a prototype (Fig. 3) on top of the passenger vehicle roof 1.85 m above the ground as shown in Fig. 1. The zoom ratio was initially set to 3.0, and the focus position was set to 30.0 m.

3.2. Results

Fig. 4 illustrates how Falcon was able to observe a curved mirror. The curved mirror was stably tracked at the center of the image, thanks to the visual feedback provided by the proposed method. We compared the images captured by the proposed system with those captured by an external camera, as shown in Fig. 5. We confirmed that the situation behind the corner was clearly visible on the image reflected by the curved mirror. Even though the external camera had a very high resolution

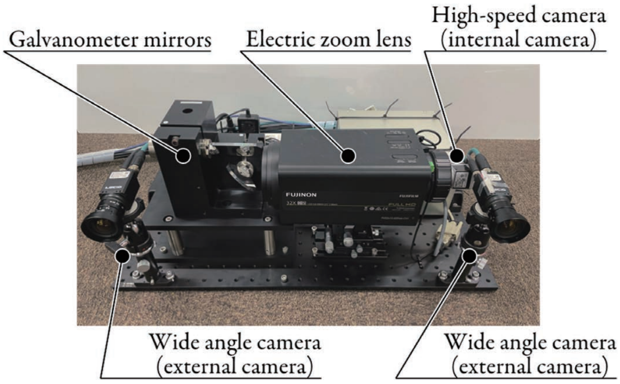

Fig. 3 A prototype of Falcon

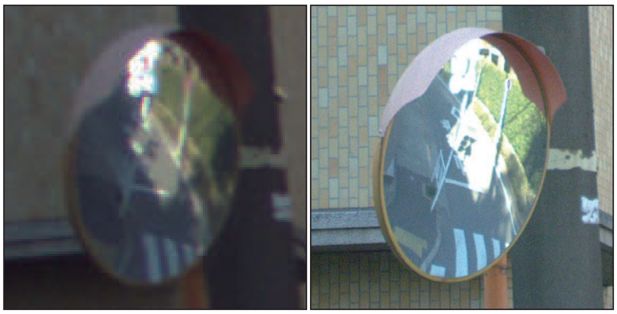
External camera Falcon

Fig. 5 Comparison of the images of the curved mirror.

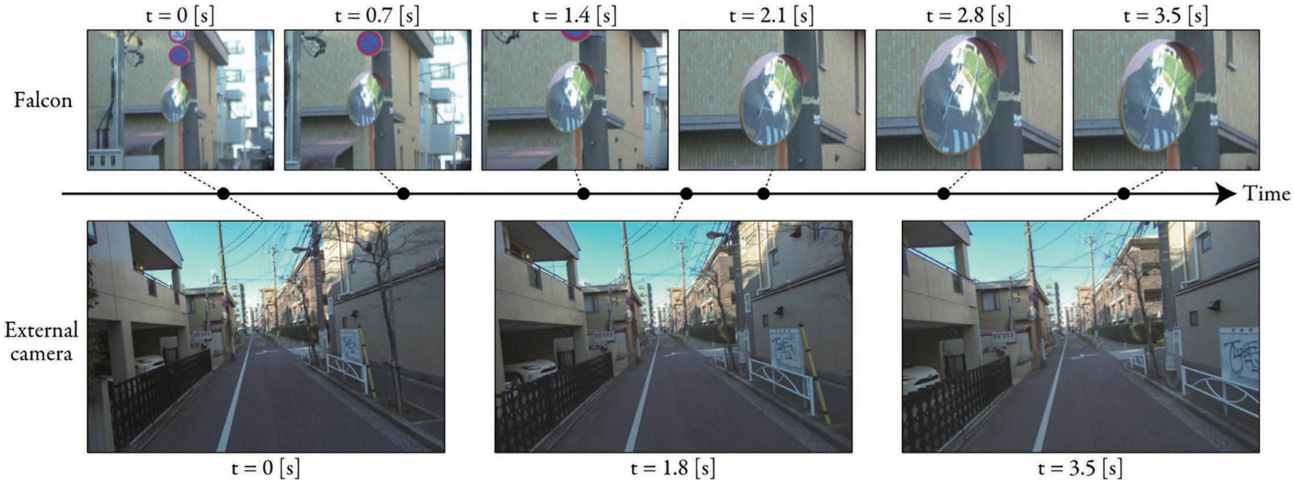

Fig. 4 Curved mirror tracking

(2880×1860), we observed that the imagery by Falcon was superior in terms of image resolution, which contributed to improving subsequent processes.

4. Conclusion

In this study, we propose an innovative active vision system composed of an electric zoom lens attached to a high-speed camera with a pair of fast-tilting mirrors for gaze control. Furthermore, we introduce a novel and accurate mapping-based calibration method for Falcon in conjunction with external cameras. We also proposed a mapping-based feedback control method for robust object tracking with minimal computational overhead. We demonstrated the system's efficacy by tracking a curved mirror on public roads and show that Falcon produced better quality imagery than a commercial high-resolution onboard camera. Future work includes the development of practical ITS applications using Falcon, such as traffic signal recognition and dangerous spot observations.